



Potential Use of Green Synthesized Al₂O₃ (Alumina) Nanoparticles from Guava Leaves (*Psidium guajava*) for the Removal of Methylene Blue from Wastewater

DEBASISH MONDAL^{1,*}, DIPANKAR MAHATA^{2,†}, KAMALA MANDY HANSDA^{1,†}, SOURAV MONDAL^{1,*} and AJIT DAS^{1,2,*}

¹Department of Chemistry, Sidho-Kanho-Birsha University, Purulia-723104, India

²Department of Environmental Science/Studies, Department of Chemistry, Balarampur College, Purulia-723143, India

*Corresponding authors: E-mail: ajit873779@gmail.com; souravchemskbu@gmail.com

Received: 29 January 2021;

Accepted: 2 April 2021;

Published online: 5 June 2021;

AJC-20360

Recently non-harmful nanomaterials have acquired critical significant attention in wastewater treatment containing organic pollutants especially toxic and hazardous dyes. In this regard, a low cost and eco friendly method has been investigated for the green synthesis of alumina nanoparticles (Al₂O₃ NPs). The alumina nanoparticles were synthesized using an aqueous extract of *Psidium guajava* leaf as a potential stabilizing agent. The UV-visible spectroscopy, Fourier-transform infrared spectroscopy (FTIR), X-ray diffraction (XRD), scanning electron microscopy (SEM) and energy-dispersive spectroscopy (EDS) techniques were used to characterize the synthesized nanoparticles. The absorption at 281 nm confirmed the formation of alumina nanoparticles. The FTIR spectra and XRD analysis confirmed the presence of various functional groups and crystalline structures of Al₂O₃ NPs during the synthesis. The spectrum clearly indicates the organic moieties in *Psidium guajava* extract are responsible for the biosynthesis of Al₂O₃ NPs. The surface morphology of Al₂O₃ NPs was confirmed by SEM and EDS studies. Besides this, the removal of methylene blue through adsorption and kinetic study was also reported.

Keywords: Alumina nanoparticles, Wastewater, Guava leaf extract, Methylene blue.

INTRODUCTION

In recent days, metal oxide nanoparticles have been extensively developed and used in many applications [1]. Alumina nanoparticles (Al₂O₃ NPs) have drawn remarkable attention, among all known metal oxide nanomaterials due to their antimicrobial activities, which are effective for sustainable biomedical applications [2]. Besides this, Al₂O₃ NPs are chemically bio-inert and stable towards hydrolysis [3]. In literature, a number of methods are reported for the synthesis of Al₂O₃ NPs, such as combustion [4], hydrothermal [5], sol-gel [6], microwave assisted [7], solvothermal [8] and ball milling [9]. But the above-mentioned procedure requires a long reaction time and hazardous chemical precursors for experimental work. Hence, these courses make an awful effect on the biological system. A sustainable, cost-effective and harmless to the ecosystem cycle through green combination is quite possibly the most encouraging approaches to make nanoparticles in current research conquer this issue [10-12]. "Green" approaches are one of the reliable and in expensive technology for the synthesis

stable metal nanoparticles with controlled size and shape. The key principle in the green process is the presence of biomolecules in plant parts which are responsible for the dual role of natural reducing agents and nanoparticles stabilizers [13,14].

Industrially useable organic dyes are wise materials with numerous applications, for example, food, cleansers, materials, horticulture and so on [15]. Due to their broad use, they have now made a genuine natural issue far and wide. Safe removal of these pollutant organic dyes is a significant issue since they contaminant drinking water as well as groundwater reservoirs [16,17]. Recently, various process has been adopted for the removal of organic dyes before their release in pollutant contaminated wastewaters [18]. Adsorption, absorption, membrane separation, flocculation and coagulation are some of the most applied techniques for the removal of organic pollutants from wastewater [19]. Nanoscale materials offer striking possibilities for the complete removal of organic pigments like methylene blue dye from wastewater to protect the ecosystem from water pollution. Nanoscale materials have micron to nano size and high specific surface area and diverse morphological structures.

Due to these key parameters of nanosized materials these materials, can go about as filtration media just as catalysts [20].

Photocatalytic oxidation is one of the most extensively adopted technology to degrade methylene blue at low cost. Several catalysts have been reported in literature for the degradation of methylene blue over the past decade. Among these catalysts, various heterogeneous catalysts including metal oxides have been considered as promising photocatalyst substrate for wastewater treatment. Zinc oxide, titanium dioxide, iron(III) oxide, niobium pentoxide, vanadium(V) oxide, tungsten trioxide, zirconia, *etc.* are the most frequently used photocatalyst for wastewater treatment [21,22]. Among those materials, alumina (Al₂O₃) nanoparticles have been the subject of huge examination. However, they have been ineffective for removing the toxic natural dyes from the contaminated water.

This work aims to prepare alumina nanoparticle through green protocol using *Psidium guajava* leaf extract, which acts as a potential stabilizing agent and is applied towards the removal of methylene blue from the contaminated wastewater. Having antimicrobial, antidiabetic and antimutagenic properties, *Psidium guajava* plant has been widely utilized in pharmaceuticals purposes [23,24]. The intrinsic phytochemicals such as saponins, tannins, alkaloids, steroids, flavonoids, *etc.* present in *Psidium guajava* leaf extracts actually responsible for its medical usefulness. The kinetic study of the removal of methylene blue from wastewater was also investigated and also compared the size of the nanoparticles with other reported literature.

EXPERIMENTAL

Fresh guava leaves were collected from the local area and washed several times with water to remove the foreign particles. After washing with water leaves is sun-dried to remove the moisture. Then 50 g of washed dried finely cut leaves were placed in a 250 mL beaker containing 100 mL of deionized water and boiled the mixture for 1 h on a hot plate. After boiling, the brownish colour extract solution was filtered, cool and finally stored in a refrigerator to be used for further experiments.

Preparation of aluminium oxide nanoparticles using extract: A 10 mL of leaf extract solution was stirred at 70 °C for 15 min followed by the addition of 10 mL of 0.1 M Al(NO₃)₃ and then the mixture was boiled. A deep yellow coloured paste was then collected in a ceramic crucible and then the same was heated in a muffle furnace at 500 °C for 2 h. The powder was obtained after heating and collected for characterization studies.

Adsorption studies: Alumina nanoparticles (10 mg) were dispersed for the adsorption studies in 100 mL of 50-400 mg L⁻¹ methylene blue aqueous solution. The mixture was stirred magnetically to ensure that the particles were fully suspended and that the surfaces of nanoparticles were saturated with the dye. A 10 mL solution was withdrawn after every 30 min and filtered. The UV-vis spectra of these methylene blue solutions were recorded at λ_{max} 666 nm after every 2 min. The equilibrium adsorption amount (q_e) of the adsorbent was calculated using the following equation:

$$q_e = v \times \frac{(C_0 - C_e)}{m}$$

where C₀ and C_e (mg L⁻¹) are the initial and equilibrium concentrations of the dye solution, respectively; v is the volume of the dye solution and m is the weight of nanoparticles.

Characterization: UV-visible spectrum of the alumina nanoparticles was studied on Perkin-Elmer spectrophotometer. For functional groups detection, FT-IR was studied using KBr pellet method. The spectrum was recorded in the wavelength ranging from 4000-500 cm⁻¹ using Perkin-Elmer spectrophotometer. XRD was studied to investigate the crystalline structure of alumina nanoparticle using Rigaku X-ray diffractometer with CuKα radiation (λ = 0.154 nm, 2θ = 10-80°). The SEM analysis of synthesized alumina nanoparticle was done on field emission SEM JEOL-ITHR500 microscope using a 20 KeV electron beam. The energy dispersive X-ray spectrum was recorded with JEOL-SEM operation software.

RESULTS AND DISCUSSION

Determination of the nanoparticle structures and the investigation of their chemical nature are crucial to understand how the material properties relate to their composition and structure.

UV-visible spectra: The colour changes occurred from brown (guava leaf extract) to yellow during synthesis indicates the colloidal aggregation and formation of alumina nanoparticles using leaf extract. The metal oxide alumina nanoparticles was confirmed by UV-visible analysis, which showed a characteristic absorption peak at 281 nm (Fig. 1).

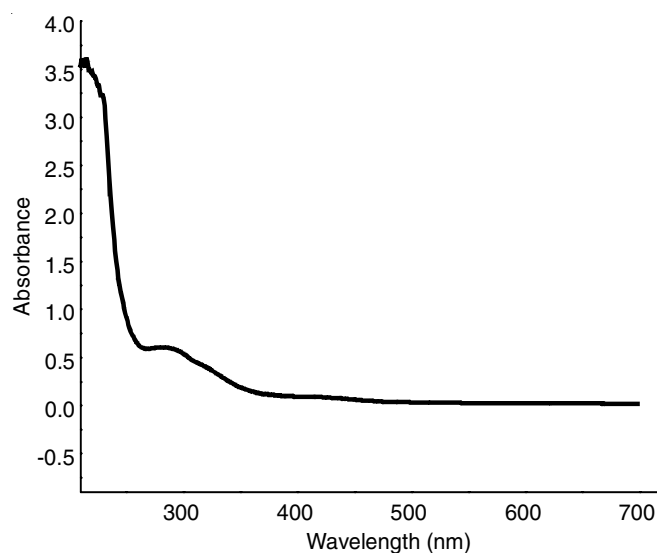


Fig. 1. UV-visible spectra of guava leaf-based alumina nanoparticle

FT-IR spectra: A broad significant peak at 3510 cm⁻¹ corresponds to the OH stretching vibrations confirmed the formation of Al-OH moieties (Fig. 2). Besides, the broad peaks at 2096.55 cm⁻¹ indicating the stretching vibrations of C≡C functional groups. Further, a peak at 1650.61 cm⁻¹ attributed to C=C aromatic stretching, while the peaks around at 1325.12 cm⁻¹ and 1149.46 cm⁻¹ attributes to the C-O and CH₂ stretching vibrations, respectively. Interestingly, the presence of a band at 630 cm⁻¹ confirmed the metal oxide bond stretching in alumina nanoparticle structure (Fig. 2).

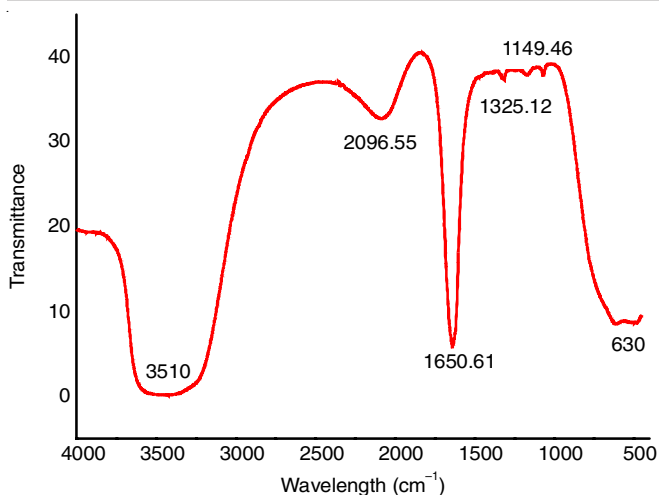


Fig. 2. FT-IR spectra of leaf-based alumina nanoparticle

XRD analysis: Fig. 3 shows the XRD pattern of the Al_2O_3 nanoparticles, which establishes their amorphous nature. There are four reflections at $2\theta = 31.9^\circ, 36.3^\circ, 39.4^\circ, 47.3^\circ, 57.1^\circ$ and 67.4° with their corresponding reflection planes of 220, 311, 222, 400, 422, 440, respectively [25], which indicates the formation of the nanoparticles. From the XRD data, it was found that the peaks are broad suggested that the crystallites have sizes in the nanometre range. The diameter (D) was calculated using Debye-Scherrer's formula:

$$D = \frac{K\lambda}{\beta \cos \theta}$$

where K is the Scherrer constant, λ is the X-ray wavelength, β is the peak width of half maximum and θ is the Bragg diffraction angle. The average crystallite size of alumina nanoparticles is estimated as ~ 32 nm. Besides, the results of the present work are compared with several works of alumina-based nanoparticles using different plant extract and displayed in Table-1.

SEM, EDX and elemental mapping analysis: From SEM images (Fig. 4a), it is evident that a fine particulate matter where the particles are elongated to a spherical shape and appear as a combination of different cotton-shaped structures. Besides this, EDX was used to determine the chemical composition or amount of the nanoparticles shown in Fig. 5. In addition with

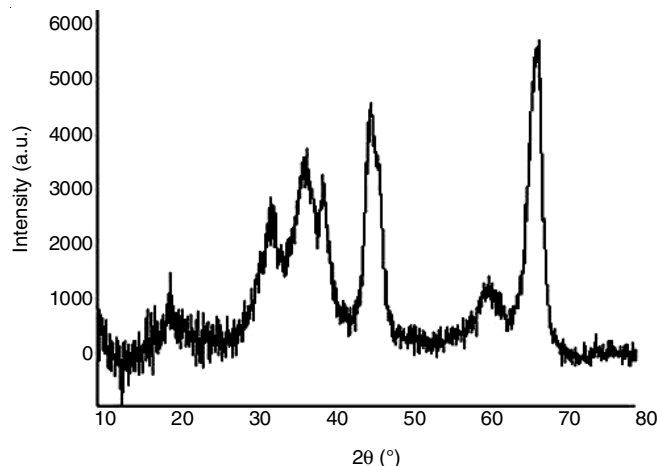


Fig. 3. XRD pattern of green synthesized alumina nanoparticle

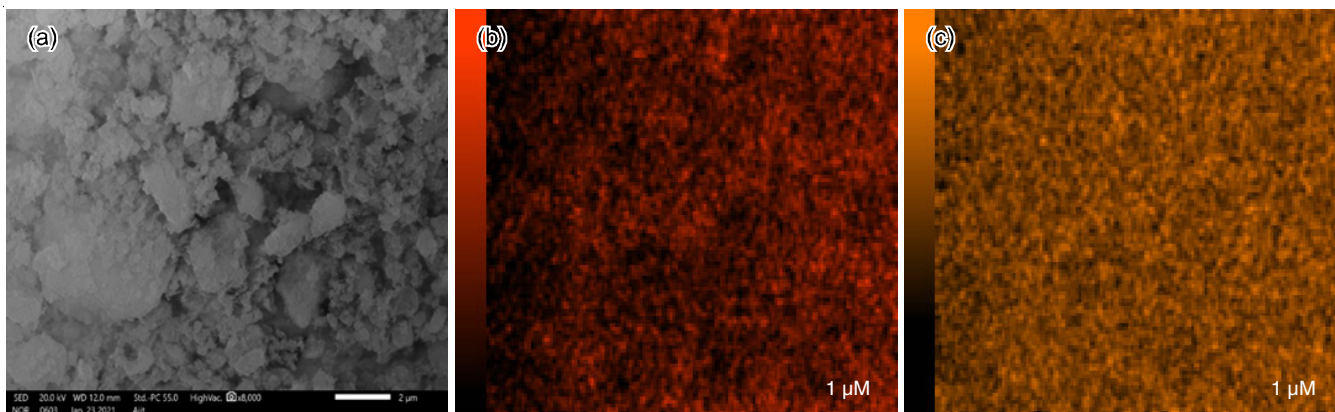
TABLE-1
SIZE OF Al_2O_3 NANOPARTICLE USING
DIFFERENT PLANT LEAVES EXTRACTS

Plant extract	Size of the nanoparticle (nm)	Ref.
Tea	50-200	[7]
Parthenium	42	[22]
<i>Prunus xyedonesis</i>	63	[23]
Rosa	53	[24]
<i>Aerva lanta</i>	50-70	[26]
<i>Psidium guajava</i> leaves	32	Present work

EDX mapping of the elements was also carried out shown in Figs. 4b and 4c. The colour images obtained from elemental mapping clearly demonstrates that the nanoparticles are basically composed of Al and O atoms. The atomic percentage of synthesized Al_2O_3 nanoparticles is shown in Table-2.

TABLE-2
ATOMIC PERCENTAGES OF GREEN
SYNTHESIZED Al_2O_3 NANOPARTICLE

Element	Line	Mass (%)	Atoms (%)
O	K	52.80 ± 0.48	65.35 ± 0.59
Al	K	47.20 ± 0.33	34.65 ± 0.24
Total		100.00	100.00
Spc_003			Fitting ratio 0.0263

Fig. 4. SEM image of synthesized Al_2O_3 (a) Elemental mapping of Al (b) and O

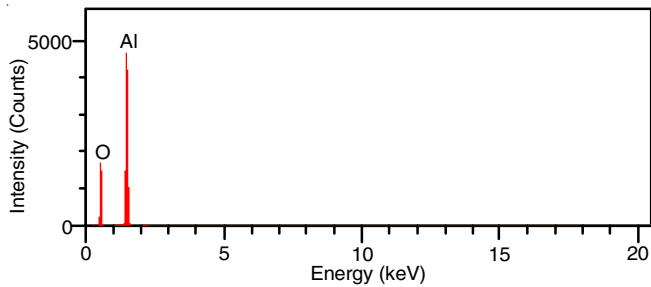


Fig. 5. EDX spectra of synthesized alumina nanoparticles

Adsorption of methylene blue: In adsorption studies using Al₂O₃ nanoparticles as adsorbent, pH has a marked effect. Fig. 6 shows that the maximum adsorption capacity was achieved at pH 9 and the initial dye concentration at this pH was 50 mg L⁻¹ at 30 °C, after that pH saturation occurs. This is probably due to the interaction between alumina surface negative charge (due to deprotonation) and the cationic structure of methylene blue.

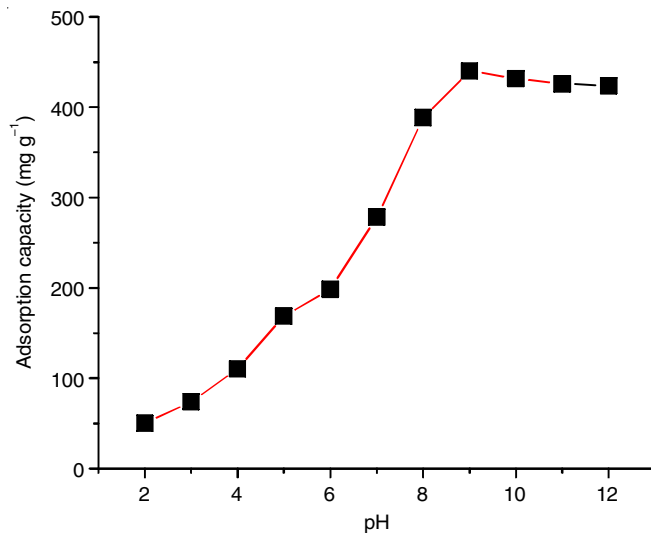


Fig. 6. Effect of pH on the adsorption of methylene blue on alumina nanoparticles at 30 °C

The absorption peaks of methylene blue in presence of 10 mg of alumina adsorbents was recorded at pH 9 at different time intervals (0-12 min). The peak at around 666 nm decreased rapidly indicating the removal of methylene blue from the solution due to the adsorption on the abundant adsorptive sites of the synthesized Al₂O₃ nanoparticles (Fig. 7).

The adsorption capacity of the adsorbent rapidly increased at the initial period of 12 min, while it became stable after 12 min as shown in Fig. 8. In this work, the adsorption of methylene blue agreeably fits with the linear form of the pseudo first-order kinetics with $R^2 = 0.99825$. The equation of pseudo first-order kinetics follows:

Pseudo-first-order kinetics:

$$\ln (q_e - q_t) = \ln q_e - k_1 t$$

where q_t is the amount (mg/g) of phosphate adsorbed at any time t and q_e is the amount of phosphate adsorbed at the equilibrium; k_1 is the equilibrium rate constant corresponds to

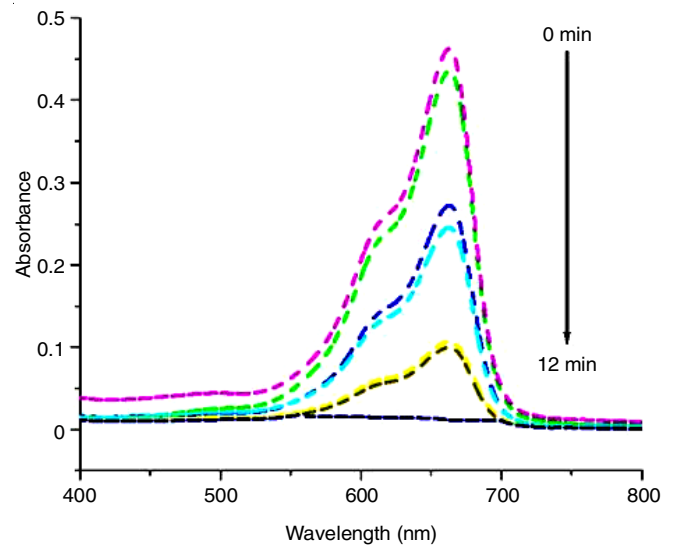


Fig. 7. UV-visible spectra of removal of methylene blue from wastewater at different interval of time

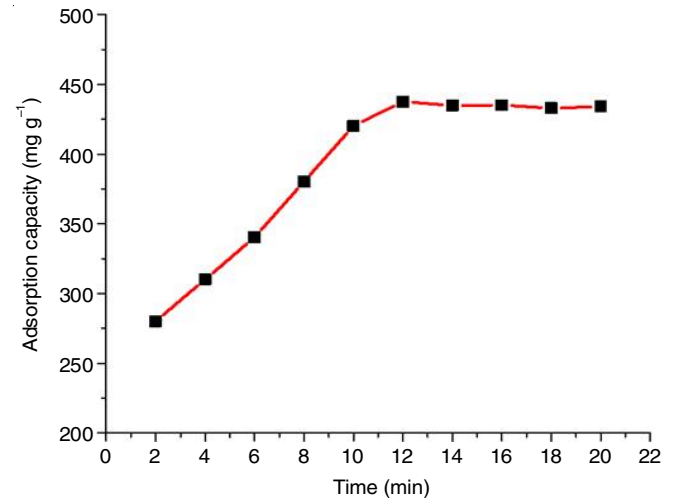


Fig. 8. Adsorption capacities of methylene blue on 10 mg of the alumina nanoparticles within 12 min at pH 9.0

pseudo-first-order kinetics. The pseudo-first-order kinetic linear plot [$\ln (q_e - q_t)$ versus t] is shown in Fig. 9.

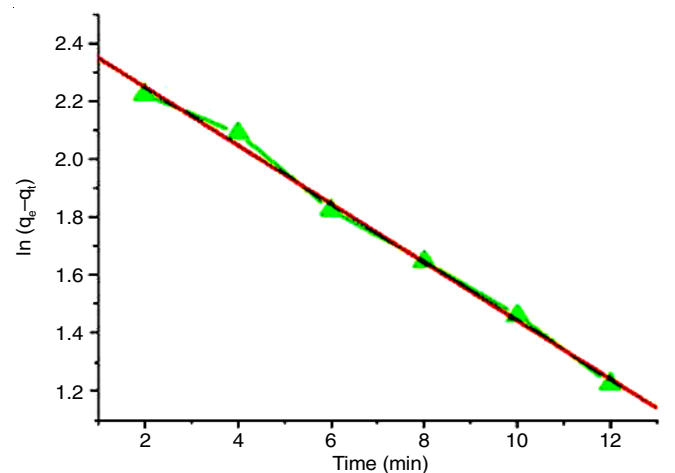


Fig. 9. The pseudo first order kinetics model

Comparative removal studies of methylene blue dye:

The removal capacities with various reported nanoadsorbents were compared with the synthesized alumina nanoparticles. The comparison studies (Table-3) clearly demonstrated that green synthesized alumina nanoparticles as adsorbents had better adsorption capacities. The reason can be attributed due to the smaller size of the prepared nanoparticles as compared to the other reported nanoparticles. Thus, from an industrial point of view, alumina nanoparticles prepared from guava leaf extract can be used as a low-cost adsorbent to remove organic pigments from contaminated wastewater.

TABLE-3
LITERATURE STATEMENT OF NANOMATERIALS
FOR THE REMOVAL OF METHYLENE BLUE

Nanoadsorbents	Adsorption capacities (mg g ⁻¹)	Ref.
Magnetic ZnO/ZnFe ₂ O ₄	37.27	[27]
ZnO	250	[28]
Iron oxide	91	[29]
TiO ₂	12.6	[30]
PANI-nickel ferrite nanocomposite	6.65	[31]
CuO	95.5	[32]
CuO/Al ₂ O ₃	91.2	[33]
Al ₂ O ₃	453.43	This work

Conclusion

In this work, alumina nanoparticles was successfully synthesized from an aqueous extract of guava leaves (*Psidium guajava*) which act as a stabilizing agent using a simple eco-friendly green approaches. The absorption peak in UV-vis spectra and visually the colour change confirmed the formation of alumina nanoparticles. An elongated to spherical morphology of alumina nanoparticles was clearly observed in SEM analysis. Moreover, alumina nanoparticles showed an excellent property for the removal of organic dyes from contaminated wastewater. It is observed that within 12 min, the adsorption capacity reached a value of 450 mg g⁻¹.

ACKNOWLEDGEMENTS

The authors thank Sidho-Kanho-Birsha University, Purulia, India for their instrumental support.

CONFLICT OF INTEREST

The authors declare that there is no conflict of interests regarding the publication of this article.

REFERENCES

- M.S. Chavali and M.P. Nikolova, *SN Appl. Sci.*, **1**, 607 (2019); <https://doi.org/10.1007/s42452-019-0592-3>
- M. Jalal, M.A. Ansari, A.K. Shukla, S.G. Ali, H.M. Khan, R. Pal, J. Alam and S.S. Cameotra, *RSC Adv.*, **6**, 107577 (2016); <https://doi.org/10.1039/C6RA23365A>
- F. Meder, S. Kaur, L. Treccani and K. Rezwani, *Langmuir*, **29**, 12502 (2013); <https://doi.org/10.1021/la402093j>
- P.A. Prashanth, R.S. Raveendra, R.H. Krishna, S. Ananda, N.P. Bhagya, B.M. Nagabhushana, K. Lingaraju and H.R. Naika, *J. Asian Ceramic Soc.*, **3**, 345 (2015); <https://doi.org/10.1016/j.jascer.2015.07.001>
- Y. Hakuta, N. Nagai, Y.H. Suzuki, T. Kodaira, K.K. Bando, H. Takashima and F. Mizukami, *Mater. Sci. Eng.*, **47**, 012045 (2013); <https://doi.org/10.1088/1757-899X/47/1/012045>
- A. Rajaieyan and M.M. Bagheri-Mohagheghi, *Adv. Mater. Sci. Eng.*, **2013**, 1 (2013); <https://doi.org/10.1155/2013/791641>
- P. Sutradhar, N. Debnath and M. Saha, *Adv. Manufact.*, **1**, 357 (2013); <https://doi.org/10.1007/s40436-013-0043-0>
- T. Chu, N. Nguyen, T. Vu, T. Dao, L. Dinh, H. Nguyen, T. Hoang, T. Le and T. Pham, *Materials*, **12**, 450 (2019); <https://doi.org/10.3390/ma12030450>
- C.B. Reid, J.S. Forrester, H.J. Goodshaw, E.H. Kisi and G.J. Suaning, *Ceram. Int.*, **34**, 1551 (2008); <https://doi.org/10.1016/j.ceramint.2007.05.003>
- A.T. Marshall, R.G. Haverkamp, C.E. Davies, J.G. Parsons, J.L. Gardea-Torresdey and D. van Agterveld, *Int. J. Phytoremed.*, **9**, 197 (2007); <https://doi.org/10.1080/15226510701376026>
- G.S. Dhillon, S.K. Brar, S. Kaur and M. Verma, *Crit. Rev. Biotechnol.*, **32**, 49 (2012); <https://doi.org/10.3109/07388551.2010.550568>
- A.K. Mittal, Y. Chisti and U.C. Banerjee, *Biotechnol. Adv.*, **31**, 346 (2013); <https://doi.org/10.1016/j.biotechadv.2013.01.003>
- H.J. Lee, G. Lee, N.R. Jang, J.H. Yun, J.Y. Song and B.S. Kim, *Nanotechnology*, **1**, 371 (2011)
- A.K. Khajuria, N.S. Bisht and G. Kumar, *J. Pharmacog. Phytochem.*, **6**, 1301 (2017).
- M. Madkour and F. Al Sagheer, *Opt. Mater. Express*, **7**, 158 (2017); <https://doi.org/10.1364/OME.7.000158>
- R. Nivedhitha and S. Velmurugan, *Int. J. Chem. Pharm. Sci.*, **6**, 18 (2015).
- M. Hao, D. Fa, L. Qian and Y. Miao, *J. Nanosci. Nanotechnol.*, **18**, 4788 (2018); <https://doi.org/10.1166/jnn.2018.15288>
- N.R. Rane, V.V. Chandanshive, R.V. Khandare, A.R. Gholave, S.R. Yadav and S.P. Govindwar, *RSC Adv.*, **4**, 36623 (2014); <https://doi.org/10.1039/C4RA06840H>
- M.M. Ibrahim, S.A. El-Molla and S.A. Ismail, *J. Mol. Struct.*, **1158**, 234 (2018); <https://doi.org/10.1016/j.molstruc.2018.01.034>
- S.G. Shinde, V.S. Shrivastava and, *J. Asian Chem. Environ. Res.*, **9**, 129 (2016).
- R.K. Upadhyay, N. Soin and S.S. Roy, *RSC Adv.*, **4**, 3823 (2014); <https://doi.org/10.1039/C3RA45013A>
- P. Raizada, J. Kumari, P. Shandilya, R. Dhiman, V. Pratap Singh and P. Singh, *Process Saf. Environ. Prot.*, **106**, 104 (2017); <https://doi.org/10.1016/j.psep.2016.12.012>
- M. Kumar, A. Mehta, A. Mishra, J. Singh, M. Rawat and S. Basu, *Mater. Lett.*, **215**, 121 (2018); <https://doi.org/10.1016/j.matlet.2017.12.074>
- X.J. Qin, Q. Yu, H. Yan, A. Khan, M.Y. Feng, P.P. Li, X.J. Hao, L.-K. An and H.-Y. Liu, *J. Agric. Food Chem.*, **65**, 4993 (2017); <https://doi.org/10.1021/acs.jafc.7b01762>
- S.K. Ramamurthy and C. Sridhar, *Int. J. Appl. Pharmaceut.*, **11**, 113 (2019); <https://doi.org/10.22159/ijap.2019v11i1.29550>
- S.A. Ansari and Q. Husain, *J. Mol. Catal. B*, **70**, 119 (2011); <https://doi.org/10.1016/j.molcatb.2011.02.016>
- M. Bystrzejewski and K. Pyrzyńska, *Colloids Surf. A Physicochem. Eng. Asp.*, **377**, 402 (2011); <https://doi.org/10.1016/j.colsurfa.2011.01.041>
- A.V. Kulkarni, A. Chavhan, A. Bappakhane and J. Chimankar, *Res. J. Chem. Environ. Sci.*, **4**, 158 (2016).
- S. Sharma, A. Hasan, N. Kumar and L.M. Pandey, *Environ. Sci. Pollut. Res. Int.*, **25**, 21605 (2018); <https://doi.org/10.1007/s11356-018-2280-z>
- A.B. Makama, A. Salmiaton, E.B. Saion, T.S.Y. Choong and N. Abdullah, *Int. J. Photoenergy*, **2016**, 2947510 (2016); <https://doi.org/10.1155/2016/2947510>
- M.R. Patil and V.S. Shrivastava, *Desalination Water Treat.*, **57**, 5879 (2016); <https://doi.org/10.1080/19443994.2015.1004594>
- M.P. Geetha, P. Pratheeksha and B.K. Subrahmanya, *Cogent Eng.*, **7**, 1783102 (2020); <https://doi.org/10.1080/23311916.2020.1783102>
- C. Bradu, L. Frunza, N. Mihalche, S.-M. Avramescu, M. Neapă and I. Udrea, *Appl. Catal. B*, **96**, 548 (2010); <https://doi.org/10.1016/j.apcatb.2010.03.019>